

DESY Summer Student Project

Bc. Jakub Boldi

(DESY summer student 2015)

Date of birth:

May 5, 1991

Nationality:

Slovak

The thermal stability of amorphous Ca-based metal alloys studied by in-situ high-energy X-ray diffraction

Area of research:

Photon Physics, Material Science

Time Frame:

July 21 – September 10, 2015

Supervisor:

Ing. Jana Michalikova

Deutsches Elektronen Synchrotron DESY

Notkestr. 85

22607 Hamburg, Germany

email: jana.michalikova@desy.de

phone: +49-408998-1741



Short description of the research project

The aim of this project was to characterize the thermal stability of structure of as-prepared metallic glass based on Ca, ($\text{Ca}_{67}\text{Al}_{33}$) and follow the evolution of its structure during the thermal loading using in-situ hard X-ray diffraction. Experiments were performed at the Petra III synchrotron at the P07 beamline in Hamburg-Germany.

Contents

1 Introduction and scientific background	2
2 Goals of the research project	2
3 Experimental part	2
3.1 Preparation of samples	2
3.2 In-situ X-ray diffraction experiments	5
4 Results and Discussion	6
5 Conclusions	9
Acknowledgement	9
Bibliography	9

1 Introduction and scientific background

Most of the materials which are today commonly used for different engineering applications are crystalline, characterized by long-range-order configuration and anisotropic properties. On the other hand there are amorphous materials, characterized by short-range-order configuration and isotropic properties. There is an intensive effort over the past decade to employ amorphous materials to engineering applications because of their unique properties, such as superior strength and hardness [1,2], excellent corrosion resistance [3], shaping and forming in a viscous state [4,5], reduced sliding friction and improved wear resistance [6], and low magnetic energy loss [7].

The formation of the first metallic glass of $\text{Au}_{75}\text{Si}_{25}$ was reported by Duwez at Caltech, USA, in 1960 [8]. Some simple binary alloys such as CaAl , PdSi , CuZr and CuHf BMGs with diameter up to 2 mm were produced and the results show that also ordinary and simple alloys could possess unusual interesting.

In this work we studied the structural behavior of Ca-based metallic glass during the heating at the P07 end-station at PETRA III synchrotron in Hamburg.

2 Goals of the research project

The purpose of in-situ X-ray diffraction (XRD) experiments was to investigate the structure of amorphous Ca-based metal alloy ($\text{Ca}_{67}\text{Al}_{33}$) in the as-prepared state and during the thermal treatment up to 500 °C with the aim to determine the crystallization temperature.

3 Experimental part

3.1 Preparation of samples

The preparation of samples contains these steps:

- Weighting of elements on a digital scale with a 10^{-3} precision, *Figure 1*.
- Ramming in die with mechanical press with maximum power up to 98000 N, *Figure 2*, the final product of this procedure is a rod with a diameter of 5 mm and height of 8 mm (it is depend on a type of elements which we have).
- Multiple remelting the master alloy in electric arc furnace in vacuum at 10^{-5} mbar, *Figure 3*.
- Producing a glass metals ribbons, *Figure 7*, via melt spinning in vacuum at 10^{-5} mbar, *Figure 4* and *Figure 5*.



Figure 1:
Weighting elements on a digital scale with a 10^{-3} precision.



Figure 2:
Ramming in the die ((1) body of die, (2) moving part) by using mechanical press (3) with maximum power 98000 N.

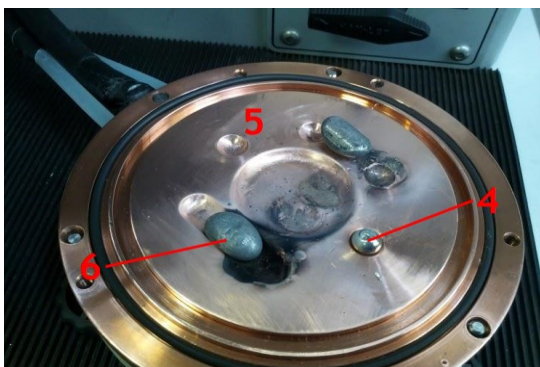
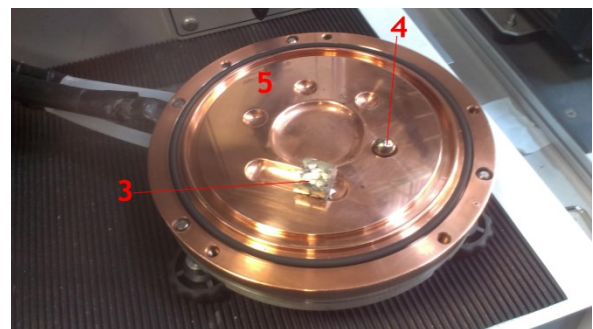
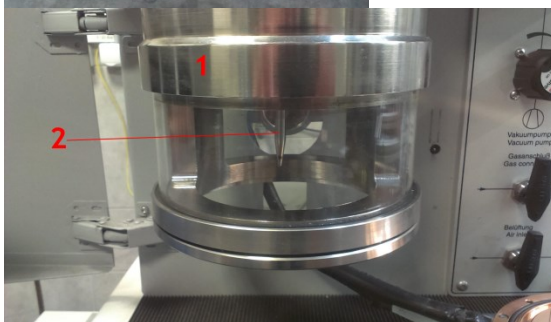


Figure 3:
Electric arc furnace, working chamber (1), W electrode (2).
Before melting (pressed mixture of elements (3) plus small Zr ball (4) on water cooled copper stand (5))
Master alloy after multiple remelting, "pills" (6).

Specifications of electric arc furnace:

- diameter of chamber: 95 mm
- volume of chamber: $1,1 \text{ dm}^3$
- melting current: 5-18 A - depends on diameter of W electrode.

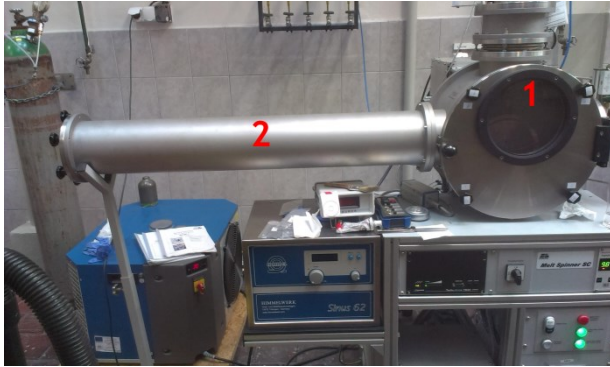


Figure4:
Melt spinner, working chamber (1), with collecting reservoir (2).

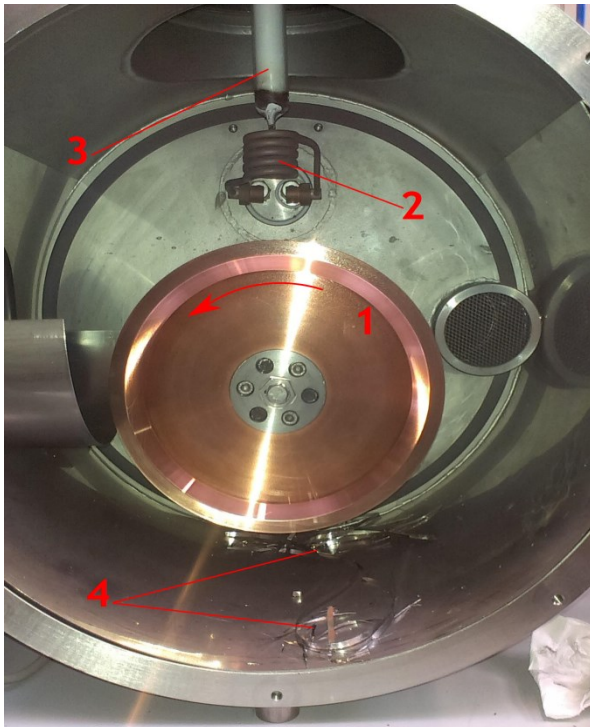


Figure5:
Melt spinner, detail view into a work chamber, Cu water cooled spinning wheel (1) with polished surface, induction heating coil (2) and quartz nozzle (3) with infill (master alloy) inside, and with BN coating of inner surface to avoid a reactions quartz with infill. On the bottom of chamber there is a ribbon (4). Temperature of “shooting” of ribbons is around 200 K above melting point of infill. System of creating vacuum: first step oil pump up to a 10^{-3} mBar and second step after reaching the desired value starts the turbomolecular pump up to a 10^{-5} mBar.



Figure 6:
Quartz nozzles: before use with cylindrical shape ending (1), before use with rectangular shape ending (2), after use with rectangular shape ending and coated inner surface with BN (3).



Figure 7:
Metallic glass in form of ribbon on a lab glass.

3.2 In-situ X-ray diffraction experiments

The measurements were carried out with the multipurpose diffraction instrument at the wiggler high-energy beamline P07 at PETRA III. Beamline P07 is dedicated to X-ray scattering experiments at photon energies in the interval from 50 keV to 200 keV. The large of penetration depth at these energies is typically several mm to cm allows the investigation of bulk materials and complex sample environments. This beamline is equipped with an on-line image-plate area detector (Perkin-Elmer 1621 detector, 2048x2048 pixels, pixel size 0.2 x 0.2 mm²) for determination of diffracted photons. In our experiment, samples were measured in quartz capillaries with 1 mm in diameter (glass thickness 0.1 mm) and exposure time was 60 seconds. The wavelength of X-ray beam was 0.125870 Å. During in-situ measurement the amorphous alloy was heated by LINKAM furnace (resist heating with water cooling). We measured in Ar atmosphere starting from the room temperature up to 500 °C with the heating rate 5 °C/min. Over 100 diffraction patterns were collected during thermal loading at selected temperatures by detector and information from those XRD patterns provided a direct evidence of ongoing structural changes. Sample temperature was controlled by a thermocouple placed inside the furnace. Diffraction patterns were integrated using Fit2D software [9]. XRD patterns are a direct evidence of structural changes occurring during thermal loading. Sample detector distance, with respect to the incoming radiation, as well as precise radiation energy were determined by fitting a standard reference LaB₆ sample.

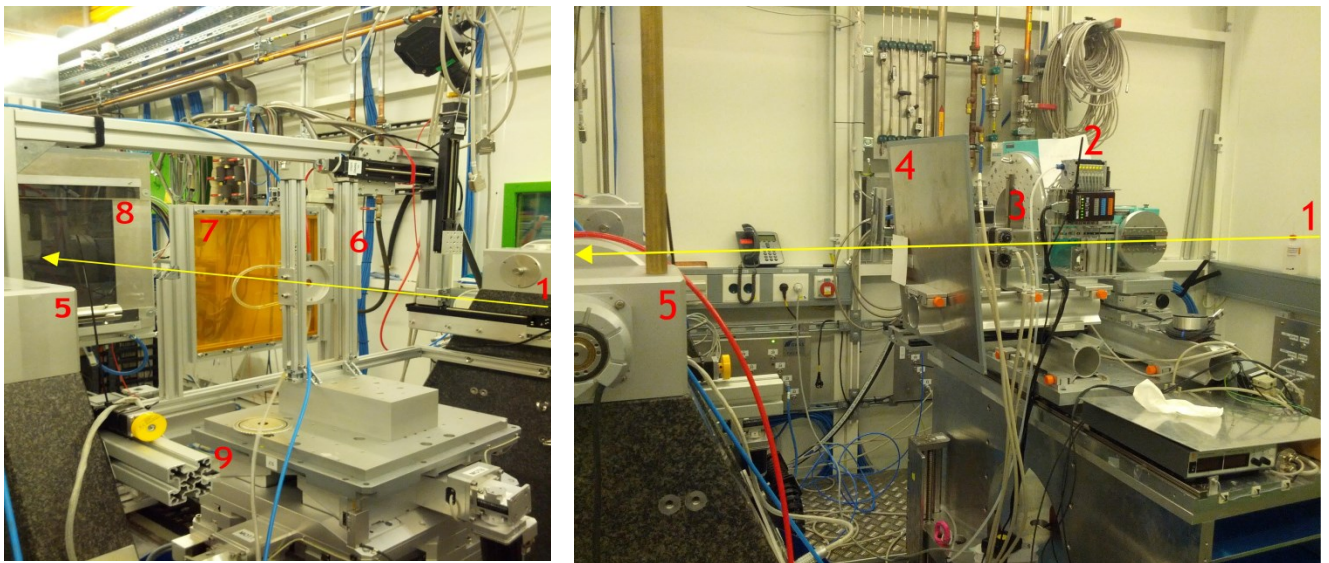


Figure 8: Beamline set-up, 1-incident beam, 2-absorbers, 3-slit, 4-pinhole, 5-marble stand, 6-LINKAM furnace, 7-beamstop, 8-Image-plate detector (Perkin-Elmer 2048x2048 pixels), and 9-goniometer.



Figure 9: Quartz capillary filled with milled metallic glass ribbon.

4 Results and Discussion

The alloy was in as prepared state amorphous, as we can see from XRD diffraction pattern shown in *Figure 10*. During in-situ measurement the amorphous sample ($\text{Ca}_{67}\text{Al}_{33}$) was heated by the LINKAM furnace starting from the room temperature up to 500 °C with heating rate 5°C/min. *Figure 11*. *Figure 12* shows series of diffraction patterns acquired during thermal loading. From the room temperature up to 250°C the alloy is in amorphous state as it can be seen from diffraction patterns, which have only one diffuse maximum. This behavior is typical for amorphous materials. At the temperature 250°C the sample starts to be crystalline, the first Bragg's peak appear.

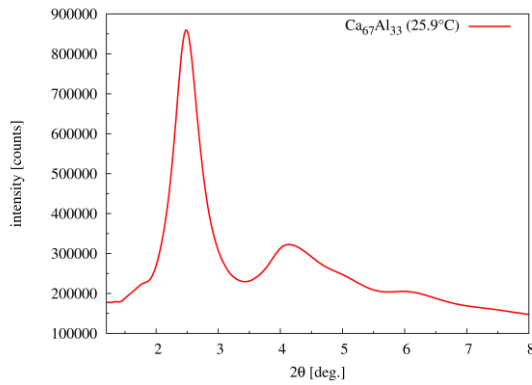


Figure 10: Radially integrated XRD pattern of as-prepared $\text{Ca}_{67}\text{Al}_{33}$ sample at temperature 25.9 °C.

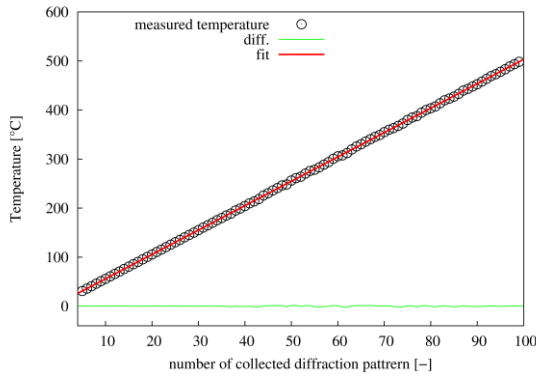


Figure 11: The temperature evaluation during the in-situ measurement.

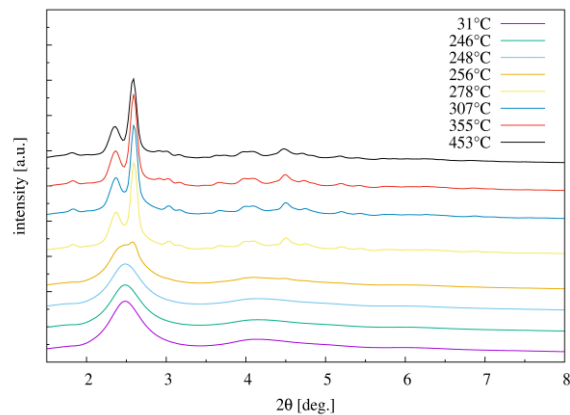


Figure 12: Selected radially integrated XRD patterns of $\text{Ca}_{67}\text{Al}_{33}$ sample. As we can see the temperature of start crystallization is 250°C.

The PDF represents variations of atomic density with respect to the mean density. In other words the PDF is measure of the probability of finding an atom at a distance from another atom and gives information about both average and the local structure of materials [10] [11]. Quantitative information about the local atomic structure can be extracted from the peaks profiles appearing on $G(r)$, for example:

- Peak position gives information about atomic bond length,
- Peak width represents length distribution of atomic bonds,
- Peak area corresponds to the average coordination number.

In the *Figure 13* shows 2D map of calculated PDF's profiles as a function of temperature. Sample exhibits amorphous structure up to temperature 250°C after that sample is crystalline. This transition we can see on PDF profiles by a significant change of oscillations which are stronger and visible up to larger distances.

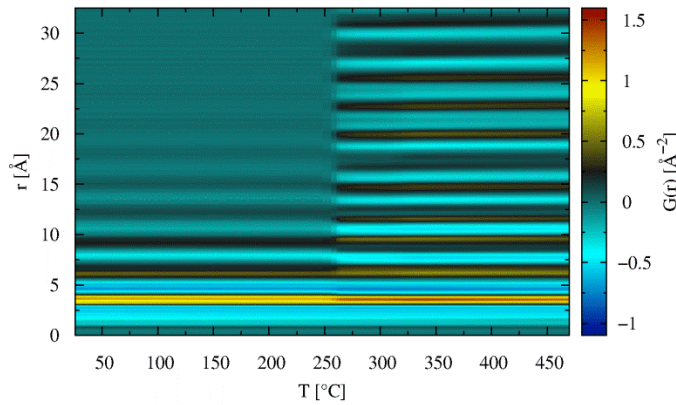


Figure 13: 2D map $G(r)$ of $\text{Ca}_{67}\text{Al}_{33}$ sample during the heat treating.

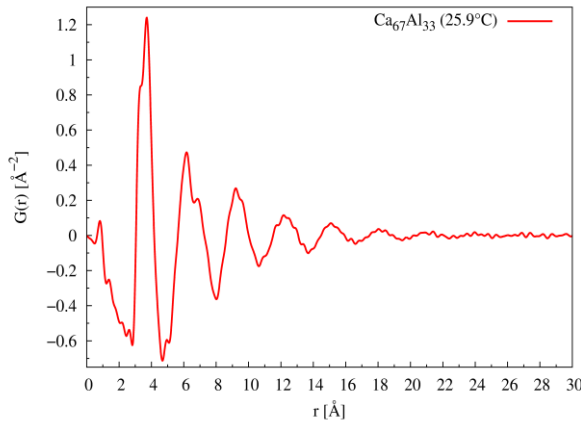


Figure 14: Total pair distribution function $G(r)$ of $\text{Ca}_{67}\text{Al}_{33}$ sample at room temperature 25.9 °C.

In case of X-ray diffraction weighting factors $w_{ij}(Q)$ (*Figure 15.*) and can be calculated using this equation:

$$w_{ij}(q) = \frac{(2 - \delta_{ij})c_i c_j f_i(q) f_j(q)}{[\sum_{k=1}^n c_k f_k(q)]^2}$$

where δ_{ij} is Kronecker delta function ($\delta_{ij}=1$ for $i=j$ and $\delta_{ij}=0$ for $i \neq j$), c and $f(q)$ are concentrations and scattering factors of atomic species of type i, j ($i, j = \text{Ca, Al}$) [10].

Table of r_{ij} -atomic radii and w_{ij} -X-ray diffraction weighting factors:

label	r_{ij} [Å]	w_{ij} [-]
Ca-Ca	3.946	0.573791
Ca-Al	3.404	0.367398
Al-Al	2.862	0.058811

The Figure 16 shows first coordination shell of $\text{Ca}_{67}\text{Al}_{33}$ sample (red curve), with fitted peaks for each contribution of atomic pair correlation using a two Gauss functions. There are two contributions from Ca-Al atomic pair correlation (green curve) and Ca-Ca atomic pair correlation (blue curve). The contribution from Al-Al atomic pair is not shown on the figure because of Al has a much smaller atomic number (13) compared to a Ca (20) and because its lower scattering power and concentration.

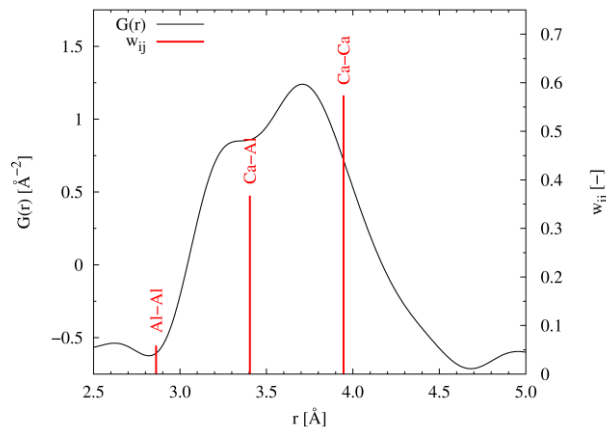


Figure 15: First coordination shell of $\text{Ca}_{67}\text{Al}_{33}$ at the room temperature (25.9°C), the vertical red lines denotes atomic separations for different atomic pairs with corresponding X-ray weights w_{ij} (calculated for $q = \text{\AA}^{-1}$ using eq. 1).

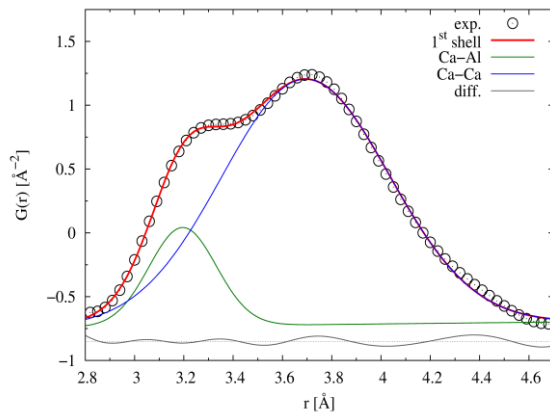


Figure 16: First coordination shell of $\text{Ca}_{67}\text{Al}_{33}$, with fitted peaks for each contribution of atomic pair correlation using a two Gauss functions.

During the heating we observed interesting behavior of the sample. Bond length (Figure 17) of Ca-Ca and Ca-Al atomic pairs is decreasing with increasing of the temperature. It is interesting because of in general with increasing temperature atomic bonds become longer.

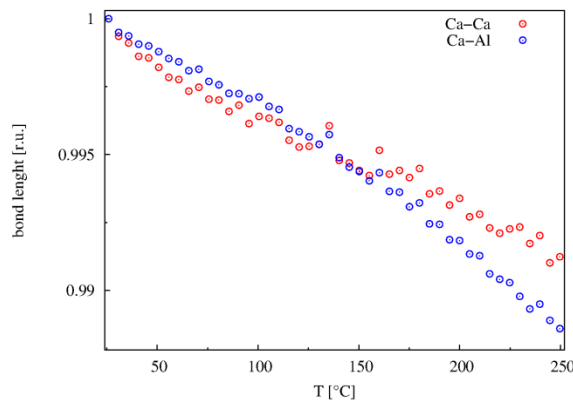


Figure 17: Temperature evolution of bond length of $\text{Ca}_{67}\text{Al}_{33}$ sample in amorphous state during the heat treatment.

5 Conclusions

We confirmed the amorphous character of as-prepared $\text{Ca}_{67}\text{Al}_{33}$ sample by X-Ray Diffraction. We estimated the crystallization temperature of sample on 250°C . Identification of crystalline phase which appears in the sample after reaching the crystallization temperature is still object of my study. Analyzing the first coordination shell appearing on the pair distribution function suggests shortening of the Ca-Ca and Ca-Al bond lengths with increasing temperature from 25°C up to 250°C .

Acknowledgement

I would like to express big thanks to my supervisor Jana Michalikova and Dr. Jozef Bednarčík, for their care, time, patience and for everything they gave me during last two months. And I also would like to acknowledge DESY for opportunity to participate in Summer Student Program 2015.

Bibliography

- [1] Inoue A, Kimura HM, Sasamori K, Masumoto T. Mater Trans JIM 1994; 35(2):85.
- [2] Hays CC, Kim CP, Johnson WL. Phys Rev Lett 2000; 84(13):2901.
- [3] Hashimoto K. In: Sakurai Y, Hamakawa Y, Masumoto T, Shirae K, Suzuki K, editors. Current topics in amorphous materials: physics and technology. Elsevier Science Publishers B.V; 1993. p. 167.
- [4] Kawamura Y, Shibata T, Inoue A, Masumoto T. Appl Phys Lett 1996; 69(9):1208.
- [5] Kawamura Y, Shibata T, Inoue A, Masumoto T. Acta Mater 1998; 46(1):253.
- [6] Wang JG, Choi BW, Nieh TG, Liu CT. J Mater Res 2000; 15(4):913.

- [7] Inoue A, Miyauchi Y, Masumoto T. Mater Trans JIM 1995; 36(5):689.
- [8] D. Turnbull. Contemporary Physics, 10:437-488, 1969.
- [9] A.P.Hammersley et al. High Press. Res.14 (1996) 235.
- [10] I. Jeong, J. Thompson, T. Proffen, S. Billinge, PDFgetX: User's Manual, Michigan State University, East Lansing, MI, USA, 2003.
- [11] T. Egami T., S. J. L. Billinge, Underneath the Bragg Peaks: Structural analysis of complex materials, Pergamon Press, Elsevier, Oxford, England, 2003.